Increased osteoblast adhesion on nanoparticulate crystalline hydroxyapatite functionalized with KRSR

Michael Nelson[1*]
Ganesan Balasundaram[2,4,*]
Thomas J Webster[2,3,4]

[1]Department of Chemical Engineering, Michigan State University, East Lansing, MI, USA; [2]Weldon School of Biomedical Engineering and [3]School of Materials Engineering, Purdue University, West Lafayette, IN, USA; [4]Present Address: Division of Engineering, Brown University, Providence, RI, USA

*These authors contributed equally to this work

Abstract: The present in vitro study created nanometer crystalline hydroxyapatite (HA) and amorphous calcium phosphate for novel orthopedic applications. Specifically, nano-crystalline HA and amorphous calcium phosphate nanoparticles were synthesized by a wet chemical process followed by hydrothermal treatment for 2 hours at 200°C and 70°C, respectively. Resulting particles were then pressed into compacts. For the preparation of control conventional HA particles (or those currently used in orthopedics with micron diameters), the aforementioned calcium phosphate particles were pressed into compacts and sintered at 1100°C for 2 hours. All calcium phosphate-based particles were fully characterized. Results showed that although there was an initial weight gain for all the compacts studied in this experiment, higher eventual degradation rates up to 3 weeks were observed for nano-amorphous calcium phosphate compared with nano-crystalline HA which was higher than conventional HA. Peptide functionalization (with the cell adhesive peptide lysine-arginine-serine-arginine [KRSR] and the non-cell-adhesive peptide lysine-serine-arginine-arginine [KSRR]) was accomplished by means of a three-step reaction procedure: silanization with 3-aminopropyltriethoxysilane (APTES), cross-linking with N-succinimidyl-3-maleimido propionate (SMP), and finally peptide immobilization. The peptide functionalization was fully characterized. Results demonstrated increased osteoblast (bone-forming cell) adhesion on non-functionalized and functionalized nano-crystalline HA compacts compared with nano amorphous calcium phosphate compacts; both increased osteoblast adhesion compared with conventional HA. To further exemplify the novel properties of nano crystalline HA, results also showed similar osteoblast adhesion between non-functionalized nano crystalline HA and KRSR functionalized conventional HA. Thus, results provided evidence that nanocrystalline HA should be further studied for orthopedic applications.

Keywords: nanomaterials, hydroxyapatite; osteoblast adhesion; KRSR grafting

Introduction

A number of applications require bone-building agents; for example, although osteoporosis has been studied for a number of years, no current effective prevention and treatment methods exist for this disease. It is clear, however, that low bone mass is a strong predictor of future fractures and this risk occurs during the normal course of aging, during unloading of the skeleton (eg, bed-rest after surgery, lack of exercise), as a consequence of certain diseases (such as arthritis and osteoporosis), and as a side-effect of various drug therapies (eg, hormone replacements, steroids). Various countermeasures (specifically, drugs, diet, and physical activity) have been developed and studied for the prevention and treatment of clinical osteoporosis (Barbucci 2002). None have experienced overwhelming success.

For example, several major barriers exist for the use of any pharmaceutical agents to stimulate new bone formation. First, these agents can cause non-specific bone formation in areas not selectively affected with a bone disease, because these agents are often delivered in non-specific ways (such as through the mouth or directly into the

Correspondence: Thomas J Webster
Division of Engineering,
Brown University, Providence, RI 02912, USA
Tel +1 401 863 2318
Fax +1 401 863 9107
Email Thomas_Webster@Brown.edu

blood stream). Second, if delivered locally to the tissue around the area of low bone density, they rapidly diffuse to adjacent tissues which limits their potential to promote prolonged bone formation in targeted areas of weak osteoporotic bone.

In terms of material solutions (ie, implants) to treat changes in bone mass, the story is not any better. For example, orthopedic implant materials (or fixation devices) are used when changes in bone mass lead to debilitating fractures (American Academy of Orthopedic Surgeons 2004). Unfortunately, the average lifetime of current orthopedic implants is only 10–15 years (Emery et al 1997). It is the hope that new materials will repair bone non-unions quickly and effectively so that the patient can return to a normal healthy life-style and not require several implant revision surgeries in their lifetime.

One promising set of materials for both delivering drugs and to increase bone mass is calcium phosphates (Otsuka et al 1994, 1997; Nimni 1997; Ruhe et al 2003). Calcium phosphate-based biomaterials have been is use in medicine and dentistry for more than two decades (Hoexter 2002; Sammarco et al 2002). One category of calcium phosphate-based materials, hydroxyapatite, arises from its similarity to bone as it is the major inorganic component. Particularly, hydroxyapatite (HA; $Ca_{10}(PO_4)_6(OH)_2$) possesses excellent biocompatibility and is osteoconductive (Wang 2004). HA can be produced using a variety of methods such as wet chemistry (precipitation), hydrothermal techniques, sol-gel, and hydrolysis of calcium phosphates (Wang 2004). The characteristics of the resulting HA particulates have significant effects on its performance to regrow bone (Wang 2004).

One material property that may influence the ability of HA and other calcium phosphate-based materials to promote bone growth is grain size. Specifically, compared with micron grain sizes, significant evidence now exists that ceramics, metals, polymers, and composites thereof with nanometer grain sizes stimulate osteoblast (bone-forming cells) activity leading to more bone growth (Webster et al 2001; Kay et al 2002; Webster and Ejiofor 2004; Webster and Smith 2005). In addition to their ability to promote new bone growth when used as implants, it is believed that nanoparticles can be formulated to selectively attach to areas of osteoporotic (not healthy) bone by either direct attachment to weak bone to release pharmaceutical agents at the site of need or by directing them to weak bone by external signals (such as magnetic particles coated with HA) (Gupta and Gupta 2005).

As a first step in this direction, the objective of this in vitro study was to develop functionalized calcium phosphate-based nanoparticles that could in the future be used either in drug delivery or as orthopedic implants to promote bone growth. Lysine-arginine-serine-arginine- (KRSR) containing peptides were used as model functionalizing agents in this study. KRSR peptides have been shown to promote the selective adhesion of osteoblasts while, at the same time, inhibit the adhesion of soft-tissue forming cells like fibroblasts (Dee et al 1998). An interesting approach that underlies this present study is whether the nanoscale features of the underlying calcium phosphate-based materials have a significant influence on osteoblast cell adhesion due to the presence of KRSR functionalization.

Materials and methods

Materials

3-aminopropyltriethoxysilane (APTES), N,N,-dimethyl-formamide (DMF), N-succinimidyl-3-maleimido propionate (SMP), and n-hexane were purchased from Sigma-Aldrich (St Louis, MO, USA). Peptides were purchased from EZ Biolab, USA.

Synthesis of nano-amorphous calcium phosphate, nano-crystalline HA, and conventional HA compacts

The process used to synthesize the calcium phosphate-based particles is outlined below in equation 1. Specifically, HA was precipitated through a well-established wet chemical process (Wang 2004; Sato et al 2005). Concentrated ammonium hydroxide was used to maintain the reaction mixture at a pH of 10 throughout the reaction. 0.6M ammonium phosphate and 1.0M calcium nitrate were also added slowly (3.6mL/min). Calcium phosphate precipitation occurred while stirring for 20 hours at room temperature.

$$10Ca(NO_3)_2 + 6(NH_4)_2HPO_4 + 8NH_4OH \rightarrow Ca_{10}(PO_4)_6(OH)_2 + 6H_2O + 20NH_4NO_3 \quad (1)$$

For the preparation of nano-amorphous calcium phosphate, the above-mentioned precipitated particles were treated hydrothermally at 70°C for 20 hours (Sato et al 2005). The white powder thus obtained was dried under vacuum (10^{-5} Torr) prior to pressing into compacts.

For the preparation of nano-crystalline HA, the above-mentioned precipitated particles were processed hydrothermally at 200°C for 20 hours. As a result, nano-sized crystalline HA can be obtained (Balasundaram et al 2006).

The resulting particles (both amorphous calcium phosphate and nano-crystalline HA) were then separately

crushed and pressed into compacts (approximately 10 mm in diameter and 1–1.5 mm in height) via a uniaxial pressing cycle that reached up to 1 GPa over a 10-min period. For the preparation of conventional HA, the pressed nano-amorphous calcium phosphate compacts were sintered at 1100°C in air for 2 hours (with a kiln ramp rate of 22°C/min).

Degradation experiment of compacts in cell culture media

The pressed compacts (calculated amount) were incubated in Dulbecco's Modified Eagle Medium (DMEM; Gibco) cell culture media supplemented with 10% fetal bovine serum (Hyclone) and 1% penicillin–streptomycin (Gibco) at 37°C for 1–21 days to evaluate their degradation. The weight loss of the compacts were measured and recorded as the degradation profile. Standard t-tests were used to check statistical significance between means. Experiments were conducted in triplicate and repeated three times each.

Peptide synthesis

The peptide epitope KRSR (KRSRGYC) represents a model cell adhesive domain which was used in this study to develop a versatile functionalization method. KSRR (KSRRGYC) was used in the present study as a non-cell-adhesive negative control peptide. Both peptides were obtained as carboxyl-terminal acids to more than 98% purity according to the HPLC profile provided by the manufacturer.

Compact functionalization

Compact functionalization was conducted under anhydrous conditions in order to avoid surface contamination from the surrounding atmosphere and hence ensure reproducibility as well as stability of the biomolecules. The strategy of peptide immobilization (Figure 1) involved: (i) grafting of an amino-functional organosilane (APTES) onto the surface of calcium phosphate-based materials and (ii) substituting the terminal amine for a hetero-bifunctional cross-linker SMP in order to (iii) react the outer maleimide group with the peptide that possessed the terminal thiol group present in cysteine. Experimentally, functionalization of the calcium phosphate-based nanoparticles was performed according to the procedure presented in Figure 1. Silanization was carried out by immersing the compacts in a solution of APTES (1×10^{-2} M) in anhydrous hexane for 2 hours (while stirring) followed by cleaning with hexane several times. Silanized compacts were outgassed at 30°C in vacuum conditionS (10^{-5} Torr) for 4 hours and were treated with SMP (2×10^{-3} M) in N, N-dimethylformamide (DMF) for 2 hours. Compacts were cleaned with hexane several times using stirring and sonication, and were outgassed at 30°C under vacuum conditionS (10^{-5} Torr) for several hours. Peptides were immobilized onto calcium phosphate-based compacts in anhydrous DMF (1 mM) for 2 hours. Finally, compacts were washed with DMF followed by several washes with deionized water.

Surface characterization

Particle characterization

Material properties of the calcium phosphate-based particles were determined by X-ray diffraction using Cu-Kα radiation (Siemens D500 Kristalloflex; Bruker AXS Inc.), inductively coupled plasma-atomic emission spectroscopy (ICP-AES, Impact Analytical, Midland, MI, USA) to measure Ca/P ratio, nanometer particle size analyzer (COULTER LS 230; Coulter Corporation, FL, USA) to measure the mean particle size, and BET (Brunauer, Emmet, Teller) to measure agglomerate particle size. Standard techniques were followed for each of the characterization methods (Sato et al 2005).

Chemical functionalization characterization

Surface chemical functionalization was determined by X-ray photoelectron spectroscopy (XPS). XPS spectra were recorded with a Kratos Analytical spectrometer on plain and peptide functionalized compacts. Power of the non-monochromatized

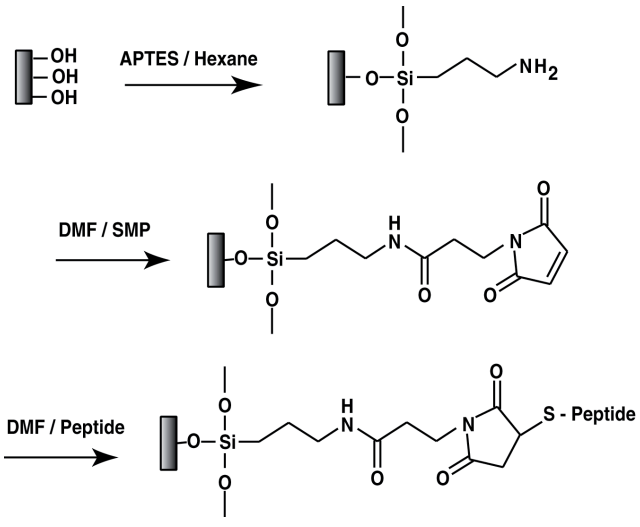

Figure 1 Reaction scheme for functionalizing peptides on calcium phosphate-based materials. In the present study, peptides were KRSR (experimental) and KSRR (negative control).
Abbreviations: APTES, amino-functional organosilane; DMF, dimethylformamide; SMP, N-succinimidyl-3-maleimido propionate.

MgKa source was 200 W with an investigated area of about 250 μm. The compacts were mounted on a sample stub with conductive carbon tape. After acquisition, fitting was then completed with software provided by Kratos Vision II; binding energy (BE) values were ± 0.2 eV.

Cell experiments

Adhesion

Compacts were sterilized under UV light for 4 hours prior to cell experiments. Human osteoblasts (bone-forming cells; CRL-11372 American Type Culture Collection, population numbers 7–8) in DMEM supplemented with 10% fetal bovine serum and 1% penicillin–streptomycin were seeded at a density of 3500 cells/cm^2 onto the compacts of interest and were then incubated in an atmosphere of 5% CO_2/95% air at 37°C for 4 hours. After the prescribed time period, substrates were rinsed in phosphate buffered saline to remove any non-adherent cells. The remaining cells were fixed with formaldehyde (Sigma), stained with Hoescht 33258 dye (Sigma), and counted under a fluorescence microscope (Leica, DMIRB; Leica Microsystems, Germany). Cell counts were completed in five fields chosen randomly per cm^2 of substrate surface area. All experiments were run in triplicate and repeated at least three separate times. Standard t-tests were used to check statistical significance between means.

Morphology

The morphology of osteoblasts adherent on the various compacts of interest to this study was characterized using a scanning electron microscope (SEM, JEOL JSM-840). For SEM analysis, compacts were first sputter-coated with a thin layer of gold-palladium using a Hummer I Sputter Coater (Technics) in a 100 mTorr vacuum argon environment for a 3-min period at 10 mA of current. Images were taken at a 5 kV accelerating voltage. Digital images were recorded using Digital Scan Generator Plus (JEOL) software.

Results

Material synthesis

Particle synthesis

Nano-amorphous calcium phosphate, nano-crystalline HA, and conventional HA particles were successfully synthesized. Material properties of the nano-amorphous calcium phosphate, nano-crystalline HA, and conventional HA particles are summarized in Table 1. Specifically, X-ray diffraction provided evidence of only one material phase in both nano-crystalline HA and conventional HA, while no crystalline phases were determined for the nano-amorphous calcium phosphate particles. BET provided evidence that nano-crystalline HA and nano-amorphous calcium phosphate had 31 and 13 nm particle sizes, respectively, while conventional HA possessed a particle size of 7400 nm. All particle types significantly agglomerated into micron sizes; specifically, nano-crystalline HA and nano-amorphous calcium phosphate agglomeration sizes were 5.21 and 8.84 μm, respectively, while conventional HA agglomerated to 169 μm. Lastly, nano-crystalline HA and nano-amorphous calcium phosphate particle shapes were irregular while conventional HA possessed cylindrical shapes.

Compact synthesis

As expected, when the aforementioned particles were compacted, SEM analysis provided evidence of increased nanometer surface roughness for the nano-amorphous calcium phosphate compared with nano-crystalline HA; compacts of nano-crystalline HA appeared more rough than conventional HA compacts (Figure 2). The specific surface area of nano-amorphous calcium phosphate (Figure

Table 1 Summary of material properties of nano-amorphous calcium phosphate, nano-crystalline HA, and conventional HA

Characterization	Nano-amorphous calcium phosphate	Nano crystalline HA	Conventional HA
Crystalline phase	–	HA	HA
Ca/P ratio	1.66	1.61	1.63
BET surface area (m^2/g)	142.11	62.165	0.26
(Crystallite or particle size [nm])	(13)	(31)	(7400)
Agglomerate particle size [μm]	8.78	4.84	120
(Median [μm])	(8.84)	(5.21)	(169)
Particle morphology	Irregular shape	Irregular shape	Cylindrical
Degradation[a]	High (3 mg/day)	Low (2.14 mg/day)	Very low (0.29 mg/day)

[a]Degradation taken between 14 and 21 days of immersion in cell culture media.
Abbreviations: HA, hydroxyapatite.

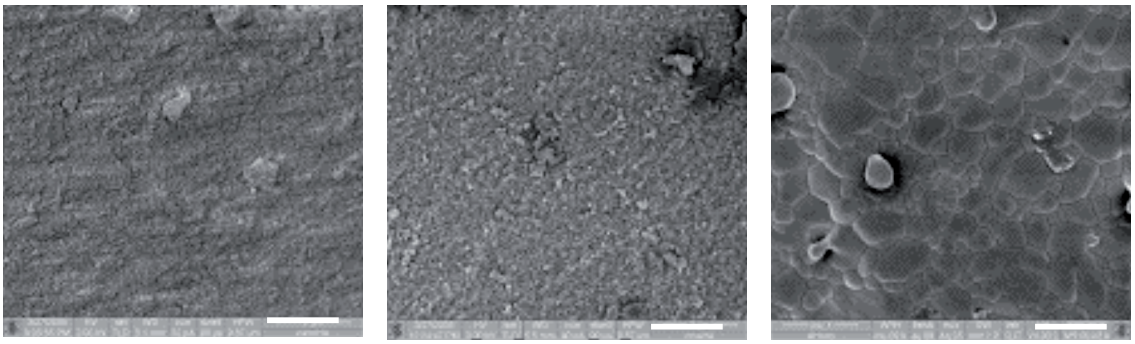

(a) Nano-amorphous calcium phosphate (b) Nano-crystalline HA (c) Conventional HA

Figure 2 Scanning electron microscopy images of calcium phosphate-based compacts. Increased compact surface roughness was observed on (a) nano-amorphous calcium phosphate compared with (b) nano-crystalline HA and (c) conventional HA. Bars = 10 µm.

2a) synthesized and processed at low temperatures was significantly larger than that of nano-crystalline HA (Figure 2b). Further, SEM analysis revealed significant morphological transformations when nano-crystalline HA was sintered to conventional HA (Figure 2c).

Degradation of compacts in cell culture media

Degradation experiments for all compacts in cell culture media showed higher degradation rates for nano-amorphous calcium phosphate compared with nano-crystalline HA, which was higher than conventional HA (Figure 3). The 3-week degradation experiment revealed a linear weight change for all compacts studied between 7 and 21 days. In all cases, the weight of the tablets initially increased before decreasing.

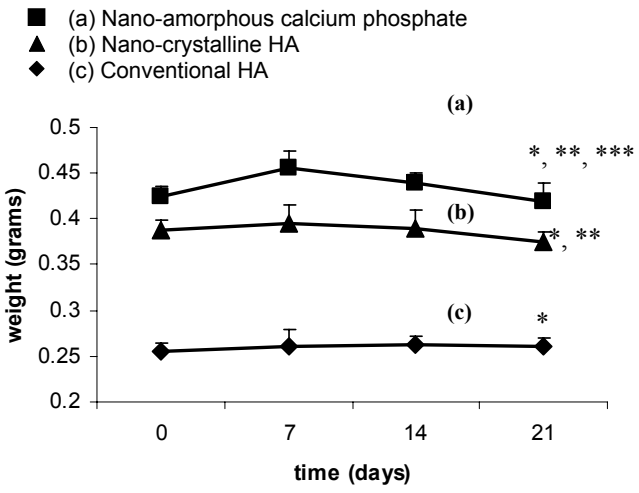

Figure 3 Degradation profile of calcium phosphate-based materials in DMEM. Data = mean ± SEM; n = 3; *p < 0.01 (compared with respective substrate at 0 days); **p < 0.01 (compared with conventional HA weight loss over the entire time period); and ***p < 0.01 (compared with nano-crystalline HA weight loss over the entire time period).
Abbreviations: HA, hydroxyapatite.

Specifically, nano-amorphous calcium phosphate displayed a sharp increase in weight followed by a linear weight decrease (Figure 3a). Though nano-crystalline HA showed an initial weight gain, it showed a comparatively slower degradation rate compared with nano-amorphous calcium phosphate (Figure 3b). However, conventional HA demonstrated very little increase in weight and a low subsequent degradation compared with both nano-amorphous calcium phosphate and nano-crystalline HA (Figure 3c). In particular, the weight difference among the compacts between 14 and 21 days showed that nano-amorphous calcium phosphate had 21 mg of weight loss, nano-crystalline HA had 15 mg of weight loss, and conventional HA had 2 mg of weight loss.

Chemical functionalization

The peptide sequences chosen for the biofunctionalization were KRSRGYC and KSRRGYC. Importantly, Ca 2p and P 2p peaks were found for all three plain substrates as expected. For example, as shown in Figures 4a4 and 4b4, plain (unfunctionalized) nanocrystalline HA displayed Ca 2p (350.2 eV–352.1 eV) and P 2s peaks (135.7 eV–136.5 eV), respectively. However, for the peptide-functionalized substrates, detection of these two elements was less obvious due to the outer layer of peptide functionalization (Figures 4a1–4a3 and 4b1–4b3). This provided an indication of the coverage of silane and peptide moieties on the functionalized compacts. Similar results were obtained for all compacts functionalized with the negative control KSRR peptide (data not shown).

Importantly, for the functionalized surfaces, XPS analysis further confirmed the presence of Si, N, and S, in addition to the expected Ca and P from HA. The Si 2p XPS spectrum showed one maximum component at 103.3 eV which corresponded to the typical SiO_3 bonding (Figures 5a1–5a3).

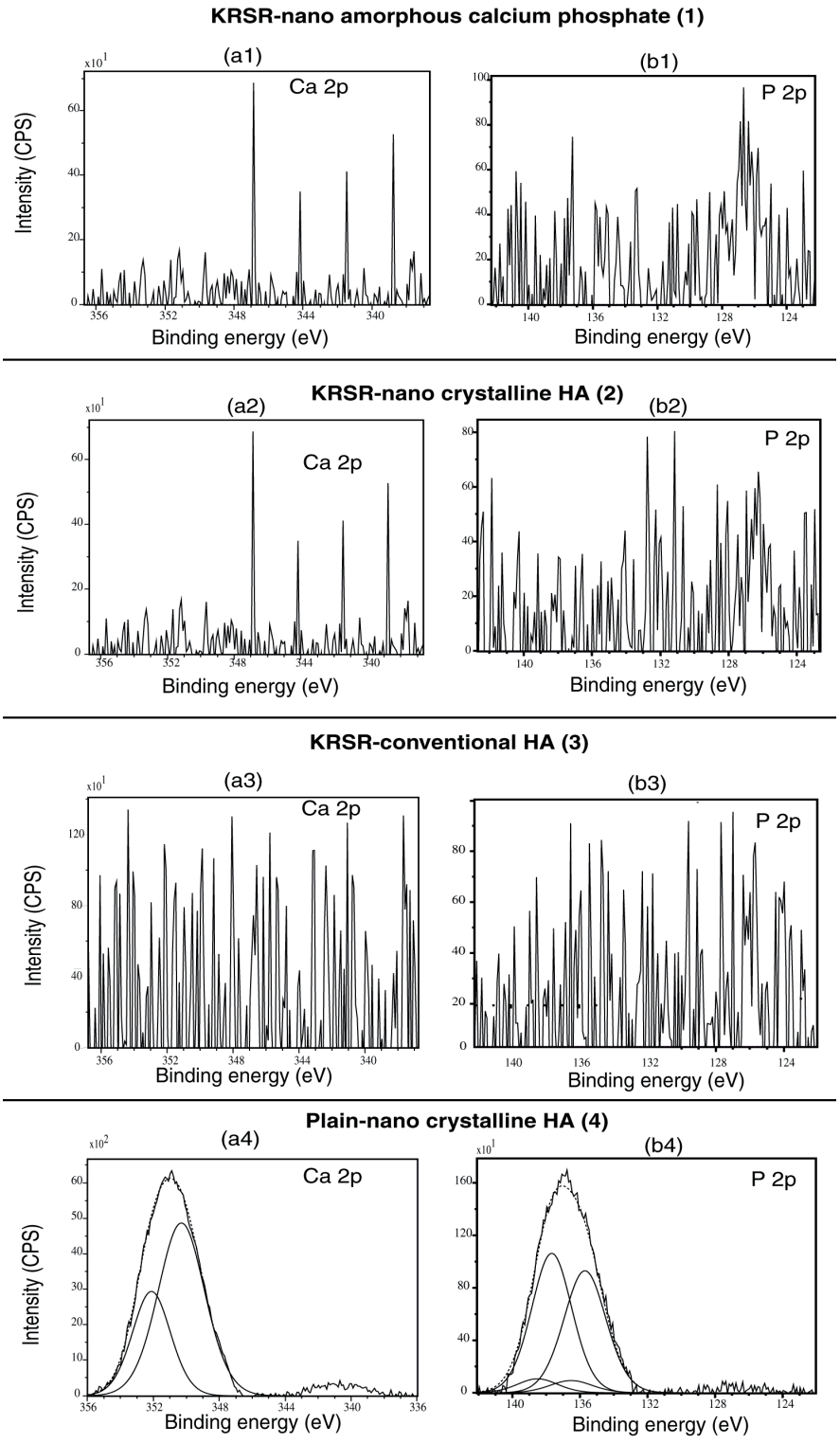

Figure 4 X-ray photoelectron spectroscopy analysis of Ca 2p, P 2p for KRSR peptide-functionalized compared with non-functionalized materials.
Abbreviations: CPS, counts per second; HA, hydroxyapatite.

In addition, the N 1s spectrum revealed two components: one of low energy (characteristic of C-NH_2 groups at 400.3 eV) and another one at 402.3 eV which can be attributed to N involved in the oxidized environment (Figures 5b1–5b3). This result may be due to some interactions between the terminal amino group and O groups near the surface. From all these observations, it is clear that the siloxane and amino acid chains were well grafted onto the surface of the particles,

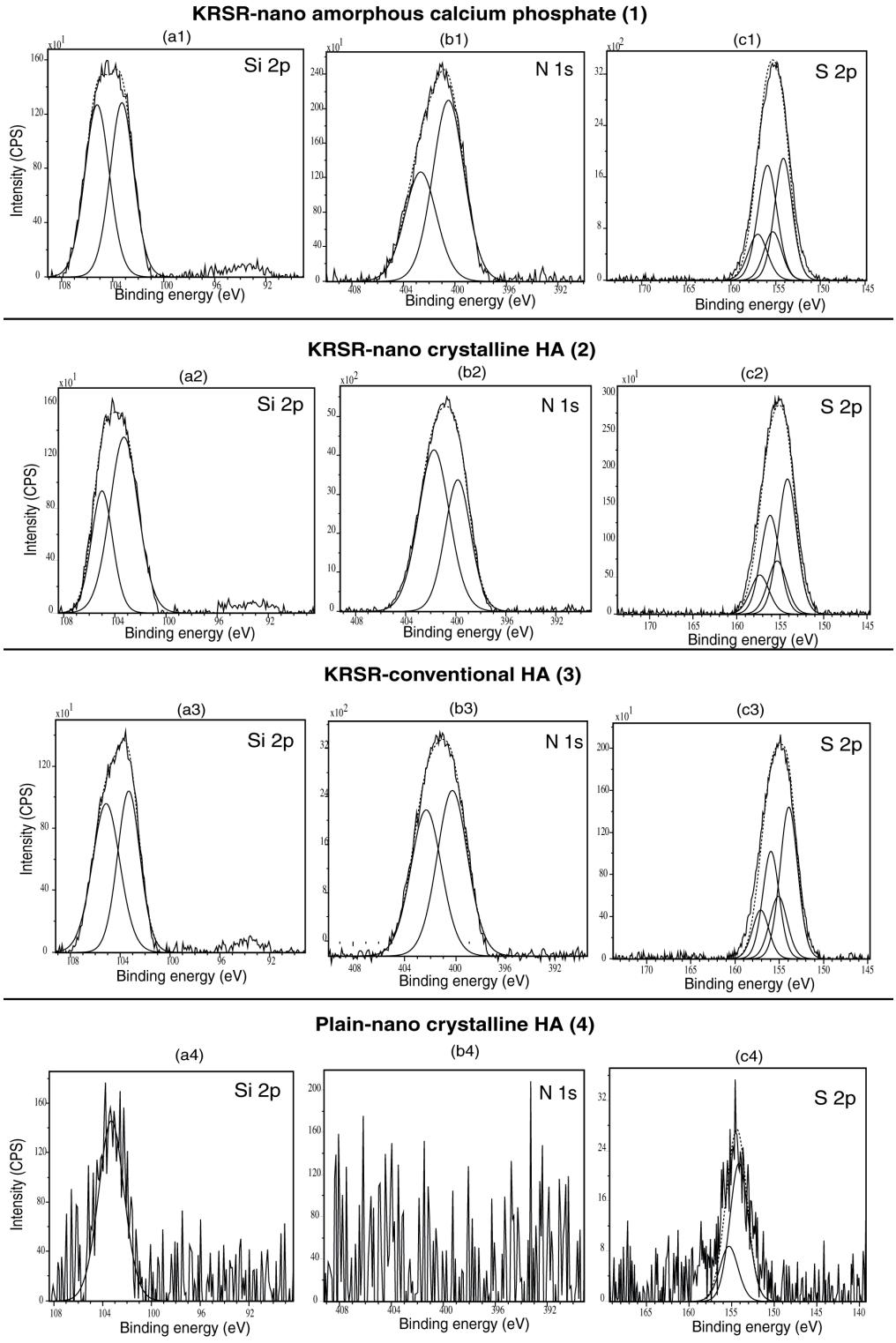

Figure 5 X-ray photoelectron spectroscopy analysis of Si 2p, N 1s, S 2p for KRSR peptide functionalized compared with non-functionalized materials.
Abbreviations: CPS, counts per second; HA, hydroxyapatite.

a critical condition for subsequent peptide attachment. After the cross-linker molecule, SMP, and peptide grafting, XPS analysis confirmed the increase in N content (Figures 5b1–5b3) due to the presence of N in every amino acid of the peptide and the presence of S (Figure 5c1–5c3) which came from the cysteine amino acid of the peptide. The presence of S 2p (which came from thiol groups of the cysteine amino acid) at 153.8 eV–155.3 eV confirmed peptide attachment.

Cell adhesion

As expected, the results obtained from cell adhesion experiments showed greater adhesion of osteoblasts to nano-amorphous calcium phosphate and conventional HA compacts functionalized with KRSR compared with either respective compacts functionalized with KSRR or the non-functionalized (plain) compacts (Figure 6). Most strikingly, osteoblast adhesion on nano-crystalline HA functionalized with KSRR was statistically higher than nano-amorphous calcium phosphate and conventional HA functionalized with KRSR (3275 cells/cm^2 for nano-crystalline HA compared with 2125 and 1030 cells/cm^2 for nano-amorphous calcium phosphate and conventional HA, respectively). The same trend was observed with the plain, non-functionalized, substrates. Furthermore, as expected, the non-adhesive peptide KRSR displayed decreased cell adhesion compared with KRSR on nano-amorphous calcium phosphate and conventional HA. Interestingly, for nano-crystalline HA, the non-adhesive, negative-control, peptide KSRR displayed similar cell adhesion compared with the KRSR peptide. Also, non-functionalized nano-crystalline HA displayed similar cell adhesion compared with KRSR functionalized on conventional HA. In this manner, this study provided the first evidence that the benefits of immobilizing KRSR on conventional HA can be matched by using non-functionalized nano-crystalline HA.

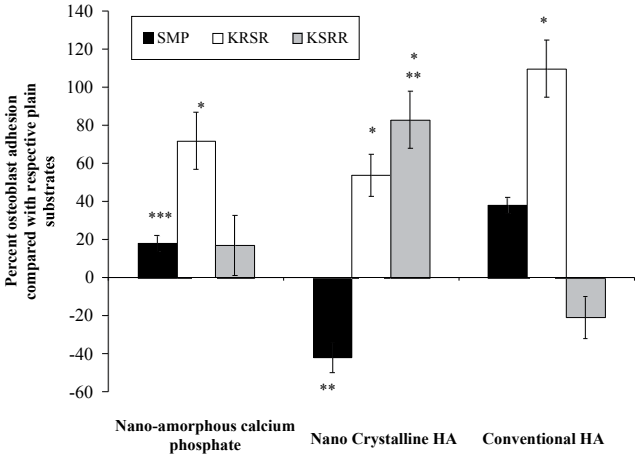

Figure 6 Increased osteoblast adhesion on nano-crystalline HA compacts functionalized with KRSR. Data = mean ± SEM; n = 3; *p < 0.01 (compared with respective plain substrate); **p < 0.01 (compared with respective conventional HA functionalization); and ***p < 0.01 (compared with respective nano-crystalline HA functionalization).
Abbreviations: HA, hydroxyapatite; SMP, N-succinimidyl-3-maleimido propionate.

Osteoblast morphology

Osteoblast morphology results confirmed quantitative results (Figure 7). Specifically, attached cells were more widespread on the nano-crystalline HA (Figure 7b) compared with nano-amorphous calcium phosphate (Figure 7a) and conventional HA (Figure 7c) after 4 hours of incubation. Osteoblasts were better spread on nano-amorphous calcium phosphate than on conventional HA.

Discussion

Interactions between cell-membrane integrin receptors and extracellular matrix proteins are often facilitated by constituent arginine-glycine-aspartic acid (RGD) amino acid sequences (Ruoslahti et al 1987; Rezania et al 1997; Xioa et al 1998; Anselme et al 2000; Schaffner et al 2003). These interactions are important for the adhesion of many cells types. Integrin-mediated cell attachment influences and regulates cell spreading, migration, proliferation, differentiation, and apoptosis (Hughes et al 1993; Saito et al 1994; Schneider et al 1994). Further, in a recent study, it was observed that decreasing the particulate size of calcium phosphate-based materials into the nanometer regime

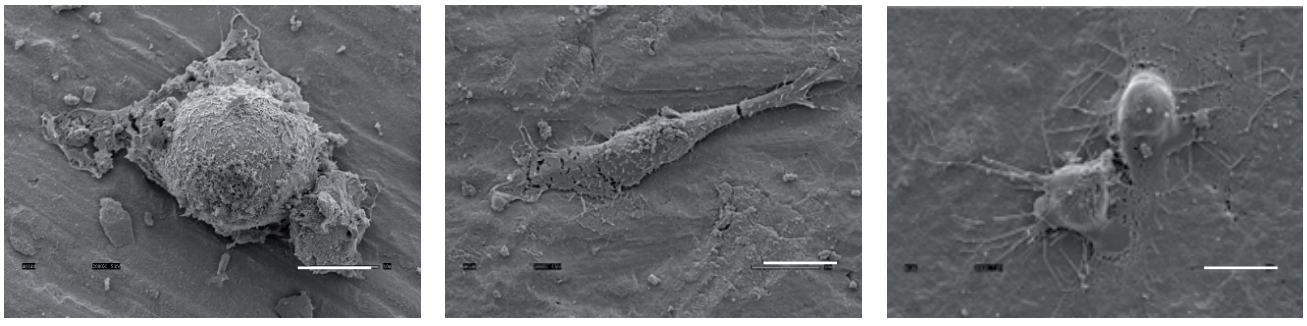

(a) Nano-amorphous calcium phosphate **(b) Nano-crystalline HA** **(c) Conventional HA**

Figure 7 Scanning electron microscopy images of osteoblasts attached to calcium phosphate-based compacts. Increased cell spreading was observed on nano-crystalline HA compared with nano-amorphous calcium phosphate and conventional HA. Bars = 10 µm.
Abbreviations: HA, hydroxyapatite.

and reducing crystallinity promoted osteoblast adhesion to the same degree as the well-established techniques of functionalizing conventional HA with RGD (Balasundaram et al 2006). This speaks to the promise nanostructured materials have in promoting osteoblast adhesion to a similar degree to that of well-established peptide immobilization techniques.

However, RGD does not completely account for all osteoblast adhesion mechanisms; other mechanisms of cell adhesion are clearly involved (Puleo et al 1992; Dalton et al 1995). For example, cell-membrane heparin sulfate proteoglycan interactions with heparin-binding sites on extracellular matrix proteins (such as fibronectin and collagen) also regulate osteoblast adhesion (Dee et al 1998). While integrin-binding peptides (for example, RGD) have been successfully immobilized on substrates to partially control osteoblast adhesion, minimal, bioactive, peptide sequences that enhance proteoglycan-mediated osteoblast adhesion (such as the presently examined KRSR) need to be considered. KRSR has recently been recognized as a prominent peptide sequence that specifically increases osteoblast adhesion compared with other cells (such as fibroblasts and endothelial cells) (Dee et al 1998). Coating implant surfaces with KRSR appears to be promising, although previous research demonstrates that KRSR, while selective for osteoblasts, does not reach the efficiency of the RGD peptide towards promoting osteoblast adhesion (Hassenbein et al 2002). Due to the importance of KRSR in mediating osteoblast adhesion, the present in vitro study focused on the covalent immobilization of the KRSR peptide onto calcium phosphate-based nanoparticles using silane derivative spacer arms.

For the first time, this paper represents an attempt to advance design criteria utilized for improving osteoblast adhesion on calcium phosphate-based materials in two ways: through the use of (i) nanometer crystalline HA particles and (ii) chemical covalent attachment techniques. Since this study demonstrated greater osteoblast adhesion on nano-crystalline HA compared with conventional (or micron grain size) HA, the present study adds nano-crystalline HA to the growing list of materials that, when created to possess constituent nanometer particulates, promote osteoblast adhesion. Since the adhesion of osteoblasts is a necessary prerequisite for subsequent cell functions (such as the deposition of calcium-containing mineral), this study also implies further enhanced functions of osteoblasts on nano-crystalline HA compared with conventional HA; clearly, however, more studies would be needed to verify this.

In this light, the present results of similar osteoblast adhesion on non-functionalized nano-crystalline HA compared with conventional HA functionalized with KRSR cannot be underestimated. Such data exemplify the potential advances that can be made in promoting osteoblast adhesion by using nanometer particles without complicated chemical immobilization techniques on conventional materials. However, the present results of increased osteoblast adhesion on plain and functionalized nano crystalline HA compared with nano-amorphous calcium phosphate contradicts that of a previous study. Specifically, a previous study highlighted greater osteoblast adhesion on non-functionalized nano-amorphous calcium phosphate compared with nano-functionalized nano-crystalline HA (Balasundaram et al 2006). This contradiction is unclear at this point and requires more experiments especially since the material property characterization results in this study matched those of the previous study (Balasundaram et al 2006). Probable reasons for this could be: (i) the hydrophilic property of the nano-amorphous calcium phosphate may have a high affinity with the positively charged KRSR moiety, thereby allowing less room for the peptide to mediate cell interactions and/or (ii) such affinity properties between KRSR and the surface might alter the peptide three-dimensional structures essential for osteoblast adhesion.

Results of this study demonstrating the successful immobilization of peptides onto calcium phosphate-based particles can be extrapolated to include other bioactive molecules and growth factors. In this manner, the techniques used in this study could allow the calcium phosphate-based particles created here to have different degrees of degradation to be utilized in a wide range of drug delivery applications; degradation can be further controlled by the inclusion of pores. Often, for orthopedic applications (such as fighting cancer or reversing osteoporosis), calcium phosphate nanoparticles are the preferred drug carrier (Coleman et al 2004).

Lastly, it is intriguing to speculate why increased osteoblast adhesion occurred on nano-crystalline HA compared with conventional HA (materials of the same crystallinity and chemistry but different particle size). Since nanophase materials are composed of particles of the same atoms but fewer (less than tens of thousands) and smaller (less than 100nm in diameter) than conventional forms (which contain several billions of atoms and have particle sizes microns to millimeters in diameter), nanophase materials have unique surface properties (Webster 2006). In this respect, nanophase materials have higher numbers

of atoms at the surface compared with bulk, greater areas of increased surface defects (such as edge–corner sites and particle boundaries), and larger proportions of delocalized surface electrons. Such altered surface properties will influence initial protein interactions that control subsequent cell adhesion (Webster 2006).

Conclusion

The results of this study provided evidence that the synthesis of nanometer particles of crystalline HA can be useful in a wide range of orthopedic applications due to their ability to increase osteoblast adhesion and have tailorable degradation properties. Results further showed the ability to functionalize peptides not only on conventional HA but also on the nanophase HA and nano-amorphous calcium phosphate compacts; critical criteria to allow attachment of other bioactive molecules for numerous applications. In particular, the cell adhesion peptide (KRSR) was used as a model peptide in this study and was immobilized onto the calcium phosphate-based compacts via aminosilane chemistry followed by a maleimide cross-linker molecule. Finally, the peptides were immobilized to the terminal maleimide group by means of covalent thiol bonding. Peptide functionalization was characterized by a well-established XPS technique. Results further demonstrated that osteoblast adhesion was similar on unfunctionalized nano-crystalline HA compared with conventional HA functionalized with KRSR. In this manner, results from this study suggest that nano-crystalline HA should be further studied for applications that necessitate bone growth.

Acknowledgments

The authors would like to thank the National Science Foundation Research Experiences for Undergraduates for financial support, Dr Debby Sherman of Purdue University for SEM pictures, and Dr Marya Liberman of University of Notre Dame for XPS measurements.

References

American Academy of Orthopedic Surgeons. 2004. Brochure [online]. Accessed 26 June 2006. URL: http:www/aaos/org/wordhtml/press/anthropl.htm.

Anselme K. 2000. Osteoblast adhesion to biomaterials. *Biomaterials*, 21:667–81.

Balasundaram G, Sato M, Webster TJ. 2006. Using hydroxyapatite nanoparticles and decreased crystallinity to promote osteoblast adhesion similar to functionalizing with RGD. *Biomaterials.* in press.

Barbucci R. 2002. Integrated biomaterials science. New York: Kluwer Academic/Plenum Publishers. p 189–689.

Coleman RE, Rubens RD. 2004. Bone metastasis. In Abeloff MD, Armitage JO, Lichter AS, et al (eds). Clinical oncology. Elsevier: Philadelphia, PA. p 1091–28.

Dalton BA, McFarland CD, Underwood PA, et al. 1995. Role of the heparin-binding domain of fibronectin in attachment and spreading of human bone-derived cells. *J Cell Sci*, 108:2083–92.

Dee KC, Andersen TT, Bizios R. 1998. Design and function of novel osteoblast-adhesive peptides for chemical modification of biomaterials. *J Biomed Mater Res*, 40:371–7.

Emery DFG, Clarke HJ, Grover ML. 1997. Stanmore total hip replacement in younger patients: review of a group of patients under 50 years of age at operation. *J Bone Joint Surg*, 79:240–6.

Gupta AK, Gupta M. 2005. Synthesis and surface engineering of iron oxide nanoparticles for biomedical applications. *Biomaterials*, 26:3995–4021.

Hassenbein ME, Andersen TT, Bizios R. 2002. Micropatterned surfaces modified with select peptides promote exclusive interactions with osteoblasts. *Biomaterials*, 23:3937–42.

Hoexter DL. 2002. Bone regeneration graft materials. *J Oral Implantol*, 28:290–4.

Hughes D, Salter D, Dedhar S, et al. 1993. Integrin expression in human bone. *J Bone Miner Res*, 8:527–33.

Kay S, Thapa A, Haberstroh KM, et al. 2002. Nanostructured polymer/nanophase ceramic composites enhance osteoblast and chondrocyte adhesion. *Tissue Eng*, 8(5):753–61.

Nimni ME. 1997. Polypeptide growth factors: targeted delivery systems. *Biomaterials*, 18:1201–25.

Otsuka M, Matsuda Y, Suwa Y, et al. 1994. A novel skeletal drug-delivery system using self-setting calcium-phosphate cement. Effects of the mixing solution volume on the drug-release rate of heterogeneous aspirin-loaded cement. *J Pharm Sci*, 83:259–263.

Otsuka M, Nakahigashi Y, Matsuda Y, et al. 1997. A novel skeletal drug delivery system using self-setting calcium phosphate cement. The relationship between in vitro and in vivo drug release from indomethacin-containing cement. *J Control Release*, 43:115–22.

Puleo DA, Bizios R. 1992. Mechanisms of fibronectin mediated attachment of osteoblasts to substrates in vitro. *Bone Miner*, 18:215–26.

Rezania A, Thomas CH, Branger AB, et al. 1997. The detachment strength and morphology of bone cell contacting materials modified with a peptide sequence found within bone sialoprotein. *J Biomed Mater Res*, 37:9–19.

Ruoslahti E, Pierschbacher MD. 1987. New perspectives in cell adhesion: RGD and integrins. *Science*, 238:491–7.

Ruhe PQ, Hedberg EL, Padron NT, et al. 2003. rhBMP-2 release from injectable poly(DL-Lactic-co-glycolicacid)/calcium-phosphate cement composites. *J Bone Joint Surg*, 85:75–82.

Saito T, Albelda S, Brighton C. 1994. Identification of integrin receptors on cultured human
bone cells. *J Orthop Res*, 12:384– 394.

Sammarco VJ, Chang L. 2002. Modern issues in bone graft substitutes and advances in bone t issue technology. *Foot Ankle Clin,* 7:19–41.

Sato M, Slamovich EB, Webster TJ. 2005. Enhanced osteoblast adhesion on hydrothermally treated hydroxyapatite/titania/poly(lactide-co-glycolide) sol-gel titanium coatings.
Biomaterials, 26:1349–57.

Schaffner P, Dard MM. 2003. Structure and function of RGD peptides involved in bone biology. *Cell Mol Life Sci*, 60:119–32.

Schneider G, Burridge K. 1994. Formation of focal adhesions by osteoblasts adhering to different substrata. *Exp Cell Res*, 21:4264–9.

Wang M. 2004. Bioactive materials and processing. In Biomaterials and tissue engineering. Shi D (ed). Heidelberg: Springer-Verlag Berlin. p 1–82.

Webster TJ, Ergun C, Doremus RH, et al. 2001. Enhanced osteoclast-like cell functions on nanophase ceramics. *Biomaterials*, 22:1327–33.

Webster TJ, Ejiofor JU. 2004. Increased osteoblast adhesion on nanophase metals: Ti, Ti6Al4V, and CoCrMo. *Biomaterials*, 25:4731–9.

Webster TJ, Smith TA. 2005. Increased osteoblast function on PLGA composites containing nanophase titania. *J Biomed Mater Res A*, 74:677–86.

Webster TJ. 2006. Proteins: structure and interactions patterns to solid surfaces. In Encyclopedia of nanoscience and nanotechnology. Schwarz JA, Contescu C, Putyera K (eds). Marcel Dekker, Inc. in press.